Bonding defects and bonding strength in liquid and amorphous $SnSe_2$

Matthieu Micoulaut

Laboratoire de Physique Théorique de la Matière Condensée, Université Pierre et Marie Curie, Boite 121

4, place Jussieu 75252 Paris Cedex 05 France

mmi@lptl.jussieu.fr

ABSTRACT

In this paper, we describe the local structure of liquid and amorphous $SnSe_2$ from First Principles Molecular Dynamics. It is found that the Sn atoms display a majority of four- and five-fold coordinations, the four-fold being made of tetrahedral and octahedral sites with defects. The rate of Sn^V is found to substantially increase when the temperature is decreased whereas the nature of the bonds (lengths, radial excursions of the bonds) appears to be quite different. The fraction of homopolar defects is also temperature dependent with a large amount of Se-Se bonds found in both liquid and amorphous systems, whereas Sn-Sn are virtually absent, a situation that contrasts with similar selenides such as $GeSe_2$.

Key words: structure of tin selenide, $SnSe_2$, First Principles Molecular Simulations.

1. INTRODUCTION

Since the pioneering work of Ovshinsy [1], chalcogenide semi-conductors have attracted a wealth of attention as they exhibit unique electrical and optical properties to be used in a wide range of applications, including electrical switching [2], data storage [3], transmission of infrared radiation [4], non-volatile memories [5]. The main origin to all these remarkable properties, already stressed fourty years ago, comes the presence of a lone pair in the electronic structure of chalcogens which lowers the band gap between valence and conduction bands under light or electrical excitation. Concerning data storage, a huge amount of interest has been devoted to materials displaying "phase-change" properties using amorphous to crystal cycles [6]. These materials are indeed used in data recording devices such as rewritable DVDs, and upcoming non-volatile memories (PRAM's). The understanding of these materials lacks a unifying viewpoint for the amorphous structures involved, and is certainly challenging. However, these amorphous systems must meet requirements for optical and electrical

properties, such as crystallization temperature, crystallization speed, and optical contrast in order to be suitable for many applications.

So far mainly tellurides have been studied for their storage properties, in particular ternary compounds containing Ge and Sb [6] as well as silver tellurides such as AgInSbTe [7]. Selenide alloys [8] have been also shown to display data storage properties based on the amorphous to crystalline phase transition. In order to optimize the search for suitable alloys displaying phase change properties, it is certainly needful to identify compositional or stoichiometric trends for important properties. Systematic studies have focused on the popular GeSbTe alloy although it has been found that alloys containing no chalcogenides at all could display phase-change properties as well [9]. Among these families of materials displaying the same kind of features, Sn-Se systems appear to lie at the boundary of phase-change properties. In fact, while $SnSe_2$ displays different material characteristics when compared to GeSbTe alloys (it shows a rather low optical contrast and a low recrystallization speed), the resistivity contrast between the crystalline and the amorphous phase amounts to 5 orders of magnitude, and the activation energy for crystallization (1.93 eV) is found to be in same range as for typical GeSbTe alloys [10]. In addition, there is a pronounced density contrast between the crystalline and the amorphous phase, which is larger than the density change typically observed for GeSbTe alloys. In this respect, $SnSe_2$ resembles but also deviates from generic phase-change material, and appears for this reason to be a very interesting system from which one can learn clues for phase-change properties.

The structure of $SnSe_2$, liquid or amorphous, is relatively unknown although neutron or X-ray diffraction has been performed in both phases [11], [12]. An insight from molecular simulations is therefore certainly timely to analyze in more detail results from experiments. Theoretical studies and especially molecular simulations have encountered problems when trying to describe the structural properties of chalcogenides from classical Molecular Dynamics [13]. In fact, the electronegativity difference between the chalcogens and atoms of Group II, IV or V is low when compared to oxides, and leads to an increased charge transfer making the use of ab initio (quantum mechanical) based electronic models necessary to describe the covalent bonding [14]. Furthermore, the low electronegativity gives rise to homopolar defects [15] whose proportions grow in the same class of compounds when moving downwards the Periodic Table. For instance, the fraction homopolar Ge-Ge bonds grows from zero [17] in GeO_2 to a non-zero fraction [18] in GeS_2 that is even increased [14] in $GeSe_2$.

Recently, liquid $SnSe_2$ has been investigated using FPMD [16] and the structure at a local and intermediate range level has been detailed. We use here the same method to describe the local structure of amorphous $SnSe_2$ with a special emphasis on the bonding defects giving rise either to homopolar bondings or to distorted polyhedral structures (tetrahedral or octahedral). We also characterize the nature of the bondings which is usually translated in terms of Peierls distorsions [19] that manifest by long and short bonds around a central atom. The present results show that it is indeed the case for $SnSe_2$.

2. ELECTRONIC MODEL

The investigation of the liquid and the amorphous phase has been undertaken using density-functional theory (DFT). The system used for the present study is made of of 120 atoms (40 Sn and 80 Se) in a cubic cell with fixed length and periodic boundary conditions. The size of the cell has been taken as 15.34 Å in order to recover the experimental density [11] of the liquid at 1173 K. The electronic structure has been described within DFT which evolves self-consistently during the motion using a generalized gradient approximation (GGA) for the exchange correlation. Valence electrons have been treated explicitly using a Becke-Lee-Yang-Parr (BLYP) norm-conserving pseudopotential accounting for core-valence interactions. The use of this exchange-correlaion functional and its related pseudopotential is rather unusual in numerical studies of chalcogenides for which a Perdew-Wang or Perdew-Burke is usually preferred [20,21], but it has been shown recently that it could provide an increased accuracy for the structural description of liquid $GeSe_2$ leading to an improved agreement of structure factors and tetrahedral arrangements [19]. Concerning the $SnSe_2$ system, the influence of the exchange-correlation has been investigated in preliminary studies, and has led to a much better agreement for the structure factor using BLYP. The wave functions have been expanded at the Γ point of the supercell on a plane-wave basis set with energy cutoff of R_c=20 Ry. An increase of the energy cutoff to 40 Ry did not showed significant differences as also found in other chalcogenides [20]. The size of the system appears to be rather well suited to address most issues related with short- and intermediate-range orders. In various liquid and amorphous Ge(Si)-Se alloys, a 120 atom simulation could indeed reproduce very accurately the structure factors obtained from neutron diffraction [14,20].

Structural analysis in the liquid phase has been performed over a trajectory of 40 ps with a time step of 0.1 fs. Subsets of 10 ps each were taken to check for the consistency of the results. The amorphous $SnSe_2$ system has been obtained by quenching the equilibrated 1iquid at 1173 K by following temperature steps of 200 K and 4 ps each. The results have on the obtained amorphous phase have been calculated from an accumulated 40 ps trajectory.

3. RESULTS & DISCUSSION

Figure 1 shows the pair distribution functions $g_{ij}(r)$ for liquid and amorphous $SnSe_2$. This allows to recover the bond distances found from XRD [12], namely 2.57 A for Sn-Se and 3.88 A for both Se-Se and Sn-Sn. Here we obtain 3.57 A and respectively 3.89 A and 4.02 A for Sn-Sn and Se-Se. First of all, it is worth to mention that the pair distribution functions in the amorphous phase display a complex shape that is usually not found in other selenides as various shoulders and small peaks can be found close to the main peaks. Obviously, new structural features emerge when the liquid at 1173 K is cooled down to room temperature: in the Se-Se partial we note that a small peak builds up at 5.54 A together with a shouldering of the main peak at 4.2 A,

whereas the "homopolar" prepeak found at 2.43 A is almost maintained. The Sn-Se shows the increase of a peak at around 6 A characteristic of some typical medium-range order elements and the Sn-Sn partial exhibits a rich variety of structural signatures: i) a small shoulder at 3.2 A arising from homopolar Sn-Sn, ii) a well-separated secondary peak close to the main peak at 3.43 A, iii) a small shoulder at around 4.75 A, and finally iv) a fairly well structured secondary peak at 6.75 A, signature of medium-range order.

A closer inspection of the structure shows that a large number of edge-sharing structures is found (15) in the system, some of them displaying an increased topological complexity because of the presence of higher coordinated tin atoms (r>4, see below). The nature of these edge-sharing motifs appears to be rather different from those found in usual chalcogenides such as $SiSe_2$. In fact, with similar Sn-Sn and Se-Se distances found from the first peak, the four-fold rings defined by the edge-sharing tetrahedra are close to a regular ($d_{Sn-Sn} = d_{Sn-Se} \sqrt{2}$) ring in terms of distances, although distorted and non-planar. Edge-sharing tendency is usually quantified from NMR data by $E^{(k)}$ functions where k=0,1,2 stands for the number of edges shared by three adjacent tetrahedral units. For instance an infinite chain will lead to 100% $E^{(2)}$ whereas silica has 100% $E^{(0)}$ because only corner-sharing connections are found in this material.
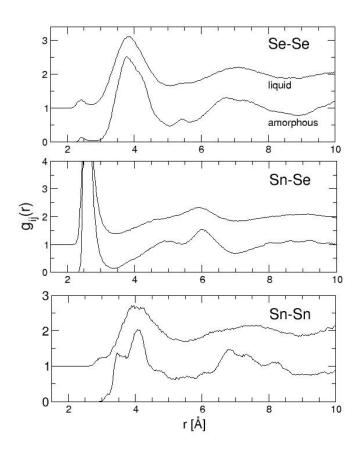

Figure 1: Pair distribution functions $g_{ij}(r)$ in the liquid (1173 K) and the amorphous phase.

In the present amorphous $SnSe_2$ system, structures of type $E^{(3)}$ are found, i.e. polyhedra which share three edges with neighbouring structures. This possibility is allowed if the coordination number of tin is larger than 4 and if three-fold Se are involved.
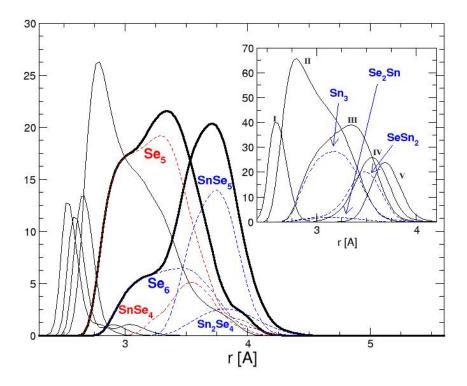

Figure 2: Neighbour distribution in amorphous SnSe2 for a centred Sn and Se, as a function of the radial distance. The curves in bold (r=4 and 5), analyzed in more details, can be split into various contributions taking into account the possibility to have homopolar bonding.

In other selenides such as $GeSe_2$ or $SiSe_2$, the local structure manifests by a strong tetrahedral ordering represented by the the sp^3 hybridization. With the presence of a more metallic element (Sn) leading to an increased electronic delocalization, a lose definition of the local geometry is expected to occur. In fact, it has been shown that the atomic neighborhood is not well defined in telluride phase-change materials [17,18]. The integration of the first peak of the Sn-Se partial yields a coordination number of r_{Sn}=4.71, larger than four, which suggests the presence of higher coordinated species. Further insight into the local structure and network topology can be obtained through the quantity $n_\alpha^l(r)$ which is the radial distribution of the average number of atoms of species α being *l*-fold coordinated, where α are Sn or Se atoms. Figure 2 represents these distributions for α=Sn and α=Se (insert). Here on can see that the first three neighbours of a Sn atom have a regular and similar distribution, whereas higher coordinated species (l=4,5,6) display a clear bimodal distribution. These

distributions can be characterized at a deeper level by looking at contributions arising from homopolar bondings (broken colored lines in Fig. 2 for l=5 and 6), i.e. for a given species α of a given coordination l corresponding to a AX_l local structure, we compute how much have X=A and how much have X $\neq$ A. Having split these distributions $n_\alpha^l(r)$, we find that for l=4, there are no homopolar bondings for Sn-centred distributions. Four-fold Sn atoms have all four Se neighbours. This furthermore means that the corresponding bimodal distribution obtained corresponds to defected octahedral units and to tetrahedral units, as also underscored by the bond angle distributions which show emerging peaks at 90°, 109° and 170° (not shown). Homopolar Sn-Sn bondings are found for l=5 and l=6, up to one in the former ($Sn(SnSe_4)$) and up to two in the latter ($Sn(SnSe_5)$ and $Sn(Sn_2Se_4)$). We finally note that i) among a given distance, the homopolar bondings correspond to the upper tail (high r domain) of the distribution and ii) the shouldering seen in the Sn-Sn pair distribution function (Fig. 1) at around 3.2 A can be clearly related to five-coordinated Sn Species ($Sn(SnSe_4)$).

Using a cutoff of 3.2 A which corresponds to the minimum of the first neighbour shell (Sn-Se partial), we find a respective fraction of 0.42, 0.43 and 0.10 for Sn^{IV}, Sn^V and Sn^{VI}, which can be compared to the numbers found [16] in the liquid (0.53, 0.32, 0.04). It suggests that higher coordinated species (r>4) build up when the temperature is decreased.
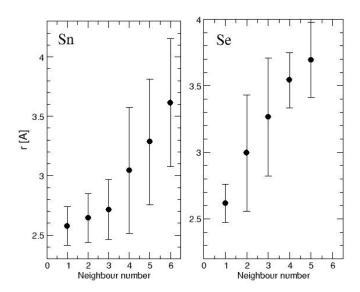

Figure 3: Mean distances (mean of the distributions given in Fig. 2) and radial excursions (error bars, second moments of the distributions given in Fig. 2) for Sn and Se in amorphous $SnSe_2$ as a function of the neighbour number.

In order to check for bonding strength, we finally consider the details of the neighbor distributions given in Fig. 2. The first moment (the average) and the second moment are computed and displayed in Figure 3 for both Sn and Se. The local bonding environment of Sn is clearly made of two contributions: 3 close neighbors having a rather well defined bond length that increases only weakly when moving from neighbor 1 (2.55 A) to neighbor 3 (2.68 A), fairly well separated from neighbors 4-6 which show an increased radial excursion (second moment). It suggests that the bond stretching interactions between two neighbors can give rise to either strong interactions (low second moments) or to weak interactions (large second moment) that do not precisely define the distance between species (with neighbour 4 in the case of Sn atoms).

4. CONCLUSION

From a structural viewpoint, amorphous tin selenide appears to be very close to the structure determined in standard phase-change materials: local structures that can have several coordination numbers (from four to six for Sn), the four-fold species being either tetrahedral or octahedral with vacancies. In addition, $SnSse_2$ displays features that are close to compounds of same Group IV chalcogenide family, namely a tendency to form edges-sharing structures which is even enhanced in the present case du to the higher coordination numbers and homopolar defects that can be quantified in much the same fashion as in $GeSe_2$. Finally, it appears that the strength of the stretching interaction can be quantified by the second moment of the neighbour distributions, and leads to bonds with a well defined length for the three first neighbours of the tin atom, and bonds with a larger radial excursion for the next neighbours.

REFERENCES

[1] S. R. Ovshinsky, Phys. Rev. Lett. **21**, 1450 _1968_.

[2] Pulok Pattanayak, S. Asokan, Europhys Lett. 75, 778 (2006).

[3] *Phase Change Materials: Science and Applications*, Eds. S. Raoux, M. Wuttig, Springer Verlag (2008)

[4] V.S. Shiryaev, J.-L. Adam, X.H. Zhang, C. Boussard-Plédel, J. Lucas, et M. F. Churbanov,   J. Non-Cryst. Solids **336**, 113 (2004);

[5] M.N. Kozicki, M. Balakrishnan, C. Gopalan, C. Ratnakumar, and M. Mitkova, IEEE Non-Volatile Memory Technology Symposium (NVMTS), D5, 1-7 (2005); J.B. Jibézède, Rev. Forfaits Av. CSE29, 124 (2007).

[6] D. Lencer, M. Salinga, B. Grabowski, T. Hickel, J. Neugebauer, M. Wuttig, Nature Materials, 7, 972 (2008)

[7] D. Milliron, S. Raoux, R. Shelby, and J. Jordan-Sweet, Nature Mater. **6**, 352 (2007).

[8] Kyung-Min Chung, D. Wamwangi, M. Woda, M. Wuttig, and W. Bensch, J. Appl. Phys. **103**, 083523 (2008).

[9] Y. Yong-Goo, Y. Dong-Seok , R. Ho-Jun, C. Woo-Seok, B. Mun-Cheol, Mater. Sci. & Eng. A 449-451, 629 (2007).

[10] M. Wuttig et al., unpublished.

[11] K. Itoh, K. Maruyama, M. Misawa, and S. Tamaki, J. Phys. Soc. Jpn. **69**, 1717 (2000)

[12] M. Popescu, F. Sava, A. Lörinczi, G. Socol, I. N. Mihailescu, A. Tomescu, and C. Simion, J. Non-Cryst. Solids **353**, 1865 (2007).

[13] P. Vashishta, R. K. Kalia, G. A. Antonio, and I. Ebbsjö, Phys. Rev. Lett. **62**, 1651 (1989) ; J. C. Mauro and A. K. Varshneya, J. Am. Ceram. Soc. **89**, 2323 (2006).

[14] C. Massobrio and A. Pasquarello, Phys. Rev. B **77**, 144207 (2008) [15] P. S. Salmon, R. A. Martin, P. E. Mason, and G. J. Cuello, Nature (London) **435**, 75 (2005).

[16] M. Micoulaut, W. Welnic, M. Wuttig, Phys. Rev. B**78**, 224209 (2008)

[17] M. Micoulaut, Y. Guissani, B. Guillot, Phys. Rev. E**73**, 031504 (2006)

[18] I. Petri, P.S. Salmon, J. Non-Cryst. Solids 293-295, 169 (2001)

[19] J. Y. Raty, V. Godlevsky, P. Ghosez, C. Bichara, J. P. Gaspard, J. R. Chelikowsky, Phys. Rev. Lett. **85**, 1950 (2000).

[18] S. Caravati, M. Bernasconi, T.D. Kuehne, M. Krack, and M. Parrinello, Appl. Phys. Lett. **91**, 171906 (2007).

[19] M. Micoulaut, R. Vuilleumier, C. Massobrio, Phys. Rev. B **79**, 214204 (2009).

[20] C. Massobrio, A. Pasquarello, and R. Car, Phys. Rev. B **64**, 144205 (2001).

Biographyies

Matthieu Micoulaut is Associate Professor at Université Pierre et Marie Curie in Paris, France. His research interest range from fundamental aspects of statistical physics : non-equilibrium dynamics, rigidity phase transition to more applied issues and materials science: phase-change materials, solid electrolytes, geomaterials. He is the author or the co-author of 70 research papers. In 2009, he has been awarded by the Stanford Ovshinsky Prize for Excellence in Non-Crystalline Chalcogenides.